Available online at www.sciencedirect.com
SCIENCE DIRECT®
Journal of Sound and Vibration 291 (2006) 503–515
JOURNAL OF SOUND AND VIBRATION
www.elsevier.com/locate/jsvi

Short Communication

# Development of a new free wake model considering a blade–vane interaction for a low noise axial fan planform optimization

Hyungki Shin, Hyosung Sun, Soogab Lee*

*School of Mechanical and Aerospace Engineering, Seoul National University, BD 311-105, San 56-1, Shilim-Dong Kwanak-Gu Seoul 151-742, Korea*

Received 16 July 2004; received in revised form 24 January 2005; accepted 6 June 2005
Available online 8 September 2005

**Abstract**

Multidisciplinary Design Optimization (MDO) is an essential part for low noise axial fan design since various parameters, such as flow rate, efficiency, noise etc., should be considered. For this reason, Response Surface Method (RSM) design technique is adopted as an axial fan design method. RSM has an advantage of choosing objective functions and constraint conditions unrestrictedly on a design space. However, RSM needs a lot of independent variables to construct a proper response surface. Thus an efficient and accurate flow analysis tool is indispensable for optimization. In an axial fan, the discrete (commonly called Blade-Passage-Frequency) components are usually dominant in the noise spectrum. Especially the blade–guide vane interaction is one of most important noise sources. In order to predict this noise component efficiently at the design stage, a new free wake model named Finite Vortex Element (FVE) is devised to simulate this blade–guide vane interaction, which is very difficult to analyze numerically in a conventional free wake model. In this new free wake model, the blade–wake–guide vane interaction is described by cutting a vortex filament when the filament collides with a guide vane. This FVE model is compared with a conventional curved vortex methodology and verified by a comparison with measured data to show its effectiveness and validity. Then FVE model is coupled with RSM to implement a low noise axial fan blade optimization. Using this method, a reduction of 8 dB(A) at 2 m from fan hub in the overall noise level is achieved while the flow rate and the efficiency are maintained as the values of the baseline blade, which implies that FVE

*Corresponding author. Tel.: +82 2 876 7383; fax : +82 2 875 4360.
*E-mail addresses:* urbung2@snu.ac.kr (H. Shin), aerosun@snu.ac.kr (H. Sun), solee@plaza.snu.ac.kr (S. Lee).

0022-460X/$ - see front matter 
doi:10.1016/j.jsv.2005.06.027

wake model coupled with RSM is very effective methodology for MDO problems such as a low noise axial fan design.


## 1. Introduction

For an axial fan, a lot of parameters such as flow rate, efficiency, noise, etc. should be considered to perform a successful design [1,2]. To satisfy this requirement, multidisciplinary design optimization (MDO) is essential part in the design stage. For this reason, response surface method (RSM) design technique is adopted as an axial fan design method. RSM has an advantage of choosing objective function and constraint condition unrestrictedly on a design space. In addition, separation of the optimization module from the analysis module promotes more efficient design environment on MDO problems such as low-noise fan design [3]. In spite of these advantages, RSM also has a disadvantage of requesting a lot of independent variables to construct a proper response surface. Therefore, an efficient and accurate flow analysis and noise prediction tool is essential parts for successful fan blade optimization. In the design stage, a free wake flow solver is proper tool. The free wake method by a curved vortex filament has already been used for the prediction of BVI noise at the rotorcraft blade successfully [4–6]. Since blade–guide vane interaction is one of most important noise sources, this phenomenon must be considered in numerical simulation so as to acquire satisfactory results for the axial fan. However, conventional free wake models cannot implement this problem. Therefore, a new free wake model, named finite vortex element (FVE) is devised in this study to analyze flow field and pressure fluctuation on blade surface during interactions of vortices with guide vanes. The effectiveness of the proposed numerical method is validated by the comparison of computational results with experimental data and then, this model is applied to optimize low noise blade planform.

## 2. Methods of approach

### 2.1. Free wake model by finite vortex elements

A conventional free wake method has many difficulties in dealing with the problem that there is an obstacle interfering with the wake such as a tower or guide vanes behind the blade. For the flow-field analysis and noise prediction in the axial fan system, blade–vane interaction is very important. To simulate this phenomenon the new free wake model is proposed, and named as FVE. In Fig. 1, an element of the different color (tone) indicates the different vortex elements, which have same vortex strength and are connected to each other. These vortex elements stream down with the flow. When these vortex filaments strike against the guide vane, they are broken down and separated into vortex ring and horse-shoe vortices (Fig. 2). These vortex rings and horseshoe vortices float inside the duct. Such a process is performed sequentially; then many vortex elements flow down between guide vanes in the duct.

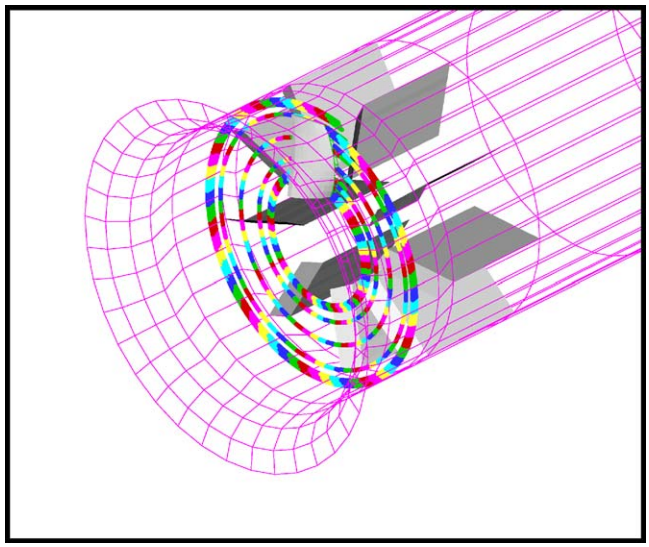

Fig. 1. Initial FVE wake geometry-an element of the different color indicate the different vorex.

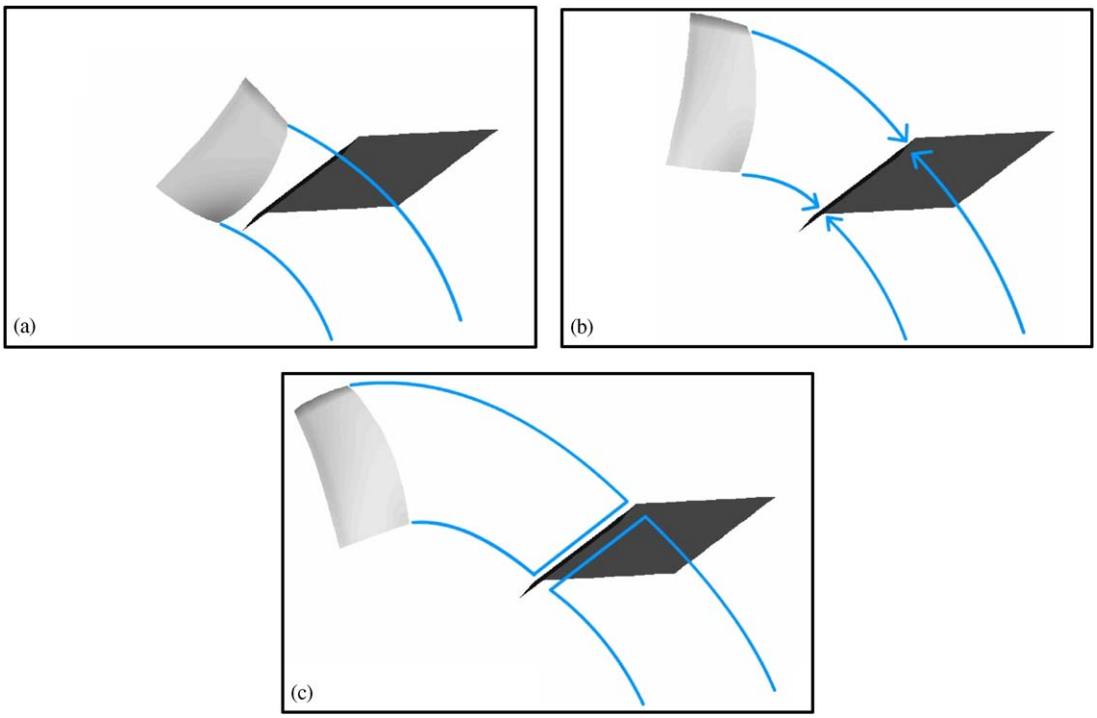


Fig. 2. Guide vane–vortex interaction; (a) before vortex filaments hit the guide vane; (b) vortex filaments strike against the guide vane (c) vortex elements are separated into vortex ring and horse-shoe vortices.

The flow of interest is in the outer region of blade where it is governed by the incompressible, irrotational continuity equation, in the blade's frame of reference, in terms of the total potential $\Phi^*$:

$$\nabla^2 \Phi^* = 0. \tag{1}$$

Following Green's identity, the general solution to Eq. (1) can be constructed by a sum of source $\sigma$ and doublet $\mu$ distributions placed on the boundary of a blade and wake:

$$\Phi^*(x,y,z) = \frac{1}{4\pi}\int_{\text{body+wake}} \mu \mathbf{n}\cdot\nabla\left(\frac{1}{r}\right) \mathrm{d}S - \frac{1}{4\pi}\int_{\text{body}} \sigma\left(\frac{1}{r}\right) \mathrm{d}S + \Phi_\infty, \tag{2}$$

where the vector $\mathbf{n}$ points in the direction of the potential jump $\mu$ which is normal to surface and positive outside of blade, and $\Phi_\infty$ is the free-stream potential.

The boundary condition for Eq. (2) can directly specify a zero normal velocity component on the surface, in which this direct formulation is called the Neumann boundary condition.

$$\nabla(\Phi + \Phi_\infty)\cdot \mathbf{n} = 0. \tag{3}$$

The second boundary condition requires that the flow disturbance should diminish far from body. Additionally, the physical condition that is called Kutta condition is necessary for the unique solution of Eq. (2).

The wake structure is made by constant vorticity contour (CVC), which is based on FVE. In this wake model, all the vortex filaments have same strength [7]. Thus the radial distance between the contour lines is a direct measure of the gradient in bound circulation along the blade. Each vorticity in the wake can be represented by

$$\boldsymbol{\gamma} = \gamma_x \boldsymbol{i} + \gamma_y \boldsymbol{j}, \tag{4}$$

where $x$ and $y$ are defined parallel to the span and to the chord of the blade, respectively.

The intensity of each component of vorticity is related to the bound circulation by

$$\gamma_x = \frac{-\Delta\Gamma(r,\psi)_{T.E}}{\Delta t} \tag{5}$$

and

$$\gamma_y = \frac{-\Delta\Gamma(r,\psi)_{T.E}}{\Delta r}, \tag{6}$$

where $\Delta r$ is the distance between each vortex release point and $\Delta t$ is time difference each azimuth angle of calculation.

The down wash by each wake element is obtained by the following equation.

$$\mathrm{d}\mathbf{w}_N = \frac{\gamma_{w,N-1}}{4\pi}\frac{\mathbf{r_1}\times\mathbf{r}_2}{|\mathbf{r_1}\times\mathbf{r}_2|}(\mathbf{r}_2-\mathbf{r}_1)\cdot\left(\frac{\mathbf{r_1}}{r_1}-\frac{\mathbf{r}_2}{r_2}\right), \tag{7}$$

where $N$ is indicative of time step.

Thus local velocity result in the following equation on each pane:

$$v_{N,\text{local}} = \omega r + f(\Gamma_{N,m}, \mathbf{w_N}) \quad \text{at global coordinates}, \tag{8}$$

where $\omega r$ is a velocity by blade rotation and $f(\Gamma_{N,m}, \mathbf{w_N})$ is a velocity by blade, duct, guide vane panels and wake.

Unsteady pressure coefficient $C_p$ applied to the acoustic analogy is represented by

$$C_{p,N} = 1 - \frac{(v_{N,\text{local}})^2}{v_{\text{ref}}^2} - \frac{2}{v_{\text{ref}}^2}\frac{\Phi_N - \Phi_{N-1}}{\Delta t}. \tag{9}$$

### 2.2. Response surface method design technique

A multiple-objective (MO) optimum design problem is solved in a manner similar to the single-objective (SO) problem. In a SO problem, the idea is to find a set of values for the design variables that, when subject to a number of constraints, yield an optimum value of the objective (or cost) function. In MO problems, the designer tries to find the values for the design variables which optimize the objective functions simultaneously, in this manner the solution is chosen from a so-called Pareto optimal set. In general, for multiobjective problems the optimal solutions obtained by individual optimization of the objectives (i.e., SO optimization) is not a feasible solution to the multiobjective problem [8].

Thus, to solve such a MO optimum design problem, response surface method is adopted as an axial fan design method. RSM is a collection of statistical and mathematical techniques useful for an optimization process. RSM incorporates collectively the design of experiments (DOE) techniques, regression analysis, and analysis of variance (ANOVA). The relationship between observations (dependent variables, the response) and independent variables (input variables) is defined as follows:

$$y = f(X). \tag{10}$$

Here, $y$ is the observed response while $X$ is the vector of $n_v$ independent variables, defined as follows:

$$X = [x_1, x_2, x_3, x_4, \ldots, x_{n_v}]. \tag{11}$$

$f(X)$ is the unknown function. The empirical model of the unknown function found via application of RSM is defined as

$$\hat{y} = \hat{f}(X), \tag{12}$$

where $\hat{f}(X)$ typically is a first- or second-order polynomial in $X$ and depends on the type of responses and input variables. Note that the random error (uncertainty) present in stochastic experimental data is implicit in both $f(X)$ and $\hat{f}(X)$. RSM employs the statistical techniques of regression analysis and ANOVA to determine $\hat{f}(X)$ through a symmetric decomposition of the variability in the observed response values. Detailed model of regression coefficient, DOE and ANOVA is referred to Refs. [8–10] because these are very long to be fully explained in this paper.

### 2.3. Acoustic prediction

The problem of noise prediction can be represented as the solution of the wave equation if the distribution of sources on the moving boundary and in the flow field is known [11]. Ffowcs-Williams and Hawkings [12] derived the governing differential equation by applying the acoustic

analogy of Lighthill [13] to bodies in motion. Farassat has developed several integral representations of the Ffowcs-Williams and Hawkings (FW-H) equation that are valid for general motions in both subsonic and supersonic flow; Farassat Formulation 1A. The solution for the acoustic pressure can be obtained by using Green's function and coordinate transformation as follows [14,15]:

$$p'(\mathbf{x},t) = p'_T(\mathbf{x},t) + p'_L(\mathbf{x},t), \tag{13}$$

$$4\pi p'_T(\mathbf{x},t) = \int_{f=0} \left[\frac{\rho_0 \dot{v}_n}{r(1-M_r)^2}\right]_{\text{ret}} \mathrm{d}S + \int_{f=0} \left[\frac{\rho_0 v_n \left(r\dot{M}_i \hat{r}_i + c_0 M_r - c_0 M^2\right)}{r^2(1-M_r)^3}\right]_{\text{ret}} \mathrm{d}S, \tag{14}$$

$$\begin{aligned} 4\pi p'_L(\mathbf{x},t) = {} & \frac{1}{c_0}\int_{f=0} \left[\frac{\dot{l}_i \hat{r}_i}{r(1-M_r)^2}\right]_{\text{ret}} \mathrm{d}S + \int_{f=0} \left[\frac{l_r - l_i M_i}{r^2(1-M_r)^2}\right]_{\text{ret}} \mathrm{d}S \\ & + \frac{1}{c_0}\int_{f=0} \left[\frac{l_r(r\dot{M}_i \hat{r}_i + c_0 M_r - c_0 M^2}{r^2(1-M_r)^3}\right]_{\text{ret}} \mathrm{d}S. \end{aligned} \tag{15}$$

Here $p'_T(\mathbf{x},t)$, $p'_L(\mathbf{x},t)$, respectively, denote the acoustic pressure due to thickness and loading, corresponding to the monopole and the dipole terms. Blade thickness rotation is modeled as monopole sources and blade surface pressure fluctuation is modeled as a dipole source term.

## 3. Results

### 3.1. Comparison of FVE wake model with curved vortex model

The noise comparison of FVE model and curved vortex model with measured data is implemented to verify the devised method. A test fan system consists of 10 blades of radius 1 m and nine outlet guide vanes. An impeller is located at the front of a duct of length 12 m. In the case of the curved vortex, panels for vane configuration cannot be employed since it is impossible to include the wake–vane interaction. This wake model is already verified in the case of BVI noise prediction at the rotorcraft field [16]. Fig. 3(a) shows the panel geometry for FVE analysis that contains blades, duct and guide vanes and Fig. 3(b) does FVE free wake geometry. The broken vortex elements float between guide vanes inside duct that depicts wake–guide vane interaction. This effect appears in the pressure fluctuation on the blade surface, which is used later for discrete noise prediction. The CVC wake structure is applied to FVE wake model as well as a curved vortex model. In this study, it provided some advantages as follows: (1) the full vortex sheet trailing from the entire span of each blade is efficiently modeled and allowed to distort freely downstream; (2) Helmholtz/Kelvin conservation laws are satisfied [16]; (c) blade–guide vane interaction is simulated automatically.

For the validation of FVE wake model, the velocity field analysis and flow rate estimation are carried out for comparison with experiments. Fig. 4(a)–(d) demonstrate a contour of an axial direction velocity at each section that illustrate at Fig. 4(A). Fig. 4(a) represents the influence of blades at velocity field, and Fig. 4(c) and (d) do an effect of guide vanes. Table 1 shows a tested

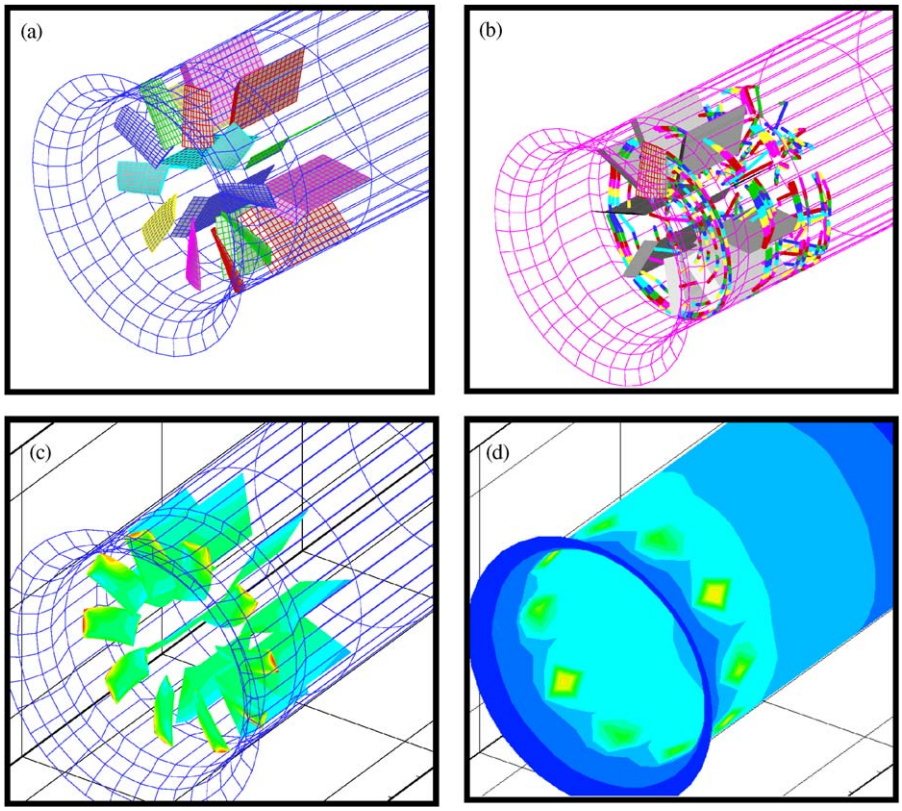


Fig. 3. (a) Panel geometry; (b) FVE wake geometry; (c) and (d) pressure distribution for noise prediction-snap shot, one time step result.

blade geometry and in Table 2, flow rate comparison shows that the discrepancies of two cases are within 5%, which is quite acceptable.

Fig. 3(c) and (d) depict a snap shot of $C_p$ distribution on all panel surfaces for noise prediction. This fan has the 149 Hz component as the first BPF, which does strongly influence noise spectrum with following harmonics up to third. Thus pressure fluctuation is calculated with a time interval of 0.00125 s for capturing 1st–3rd harmonics exactly. This time history of pressure fluctuation is shown in Fig. 5. The curved vortex analysis result has 10 peaks in one revolution that matches blade number, but FVE analysis has no periodic pattern in the pressure fluctuation result. It is explained that since blade–guide vane interaction makes the wake form complicated, the pressure fluctuation on blade surface has random pattern. Especially in a result of curved vortex analysis, the $C_p$ graph has sharp pressure spikes and $C_p$ difference is greater than that of FVE analysis.

The acoustic analogy is basically implemented in the free-field condition. But, the fan system in this study has duct and inlet cone. However, the measurement was carried out at the forward direction of the fan. The wavelength of first BPF becomes 2.2 m and inlet cone length is 0.5 m. Therefore, the reflection and diffraction of sound waves could be ignored in this study. A fan noise is measured at intervals of 2 and 4 m from its inlet as shown in Fig. 6. The calculated noise

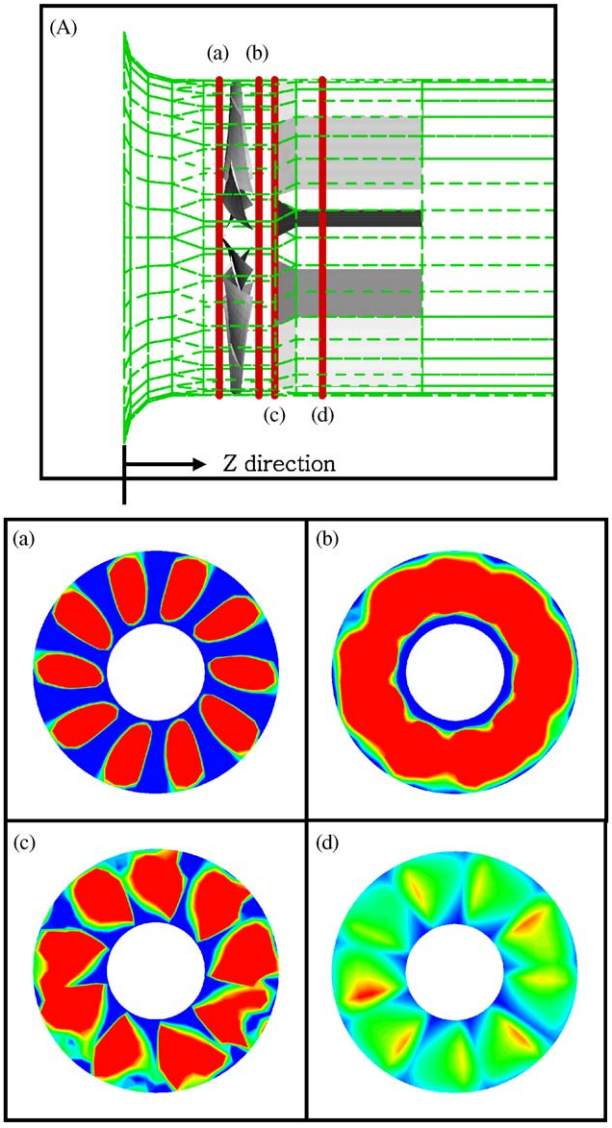


Fig. 4. Axial direction velocity contours: (A) illustrate each section where velocity field is calculated; (a) $z/R = 0.58$; (b) $z/R = 0.83$; (c) $z/R = 0.93$; (d) $z/R = 1.23$.

Table 1
Base blade geometry

| Root location | Root chord length (mm) | Taper ratio | Twist (degree) |
|---|---|---|---|
| $r/R = 0.4$ | 280 | 0.875 | 28.5 |

Table 2
Comparison of flow rate (rev/min: 890)

| Root pitch angle | Back pressure (mmAq) | Flow rate ($m^3$/min) | | |
|---|---|---|---|---|
| | | Measurements | Calculations by FVE | Difference (%) |
| 43° | 70 | 3394 | 3563 | 4.97 |
| 50° | 60 | 4799 | 4991 | 4.00 |

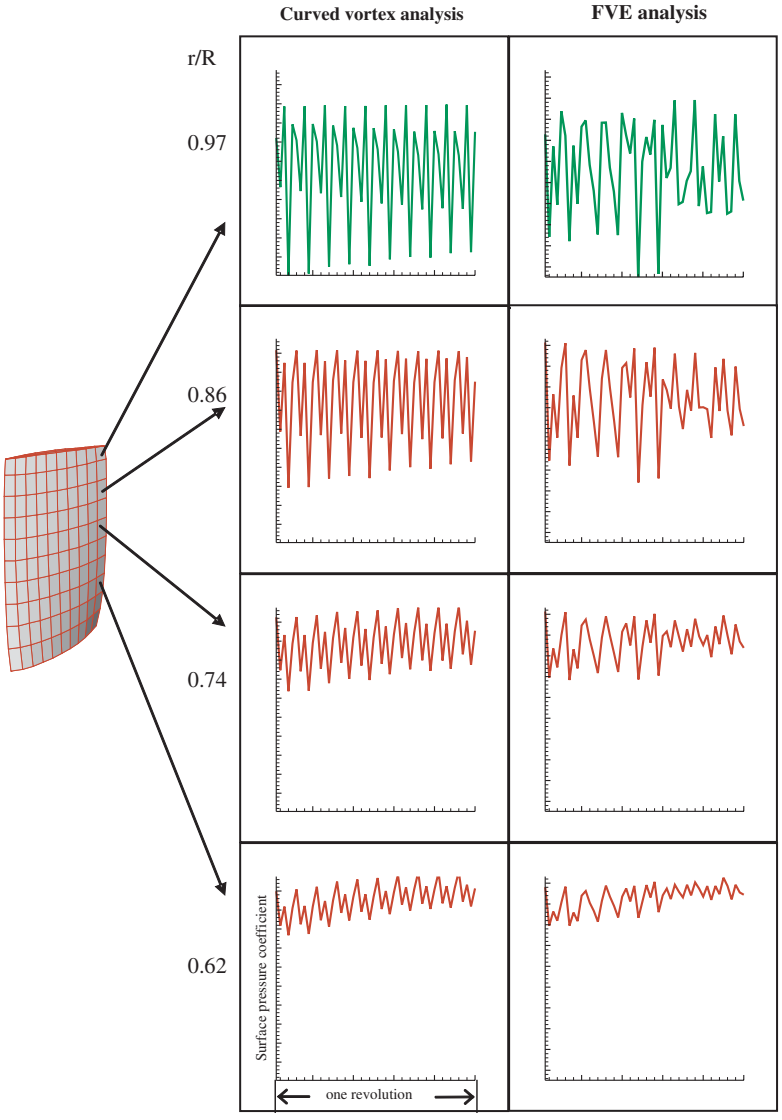


Fig. 5. Time history of upper-surface trailing-edge pressure coefficient.

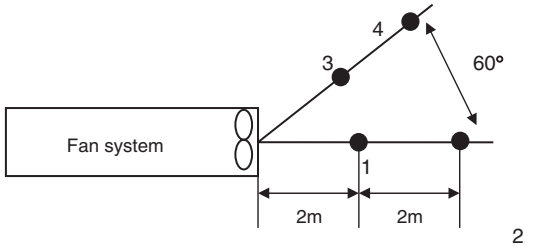


Fig. 6. Noise measurement points.

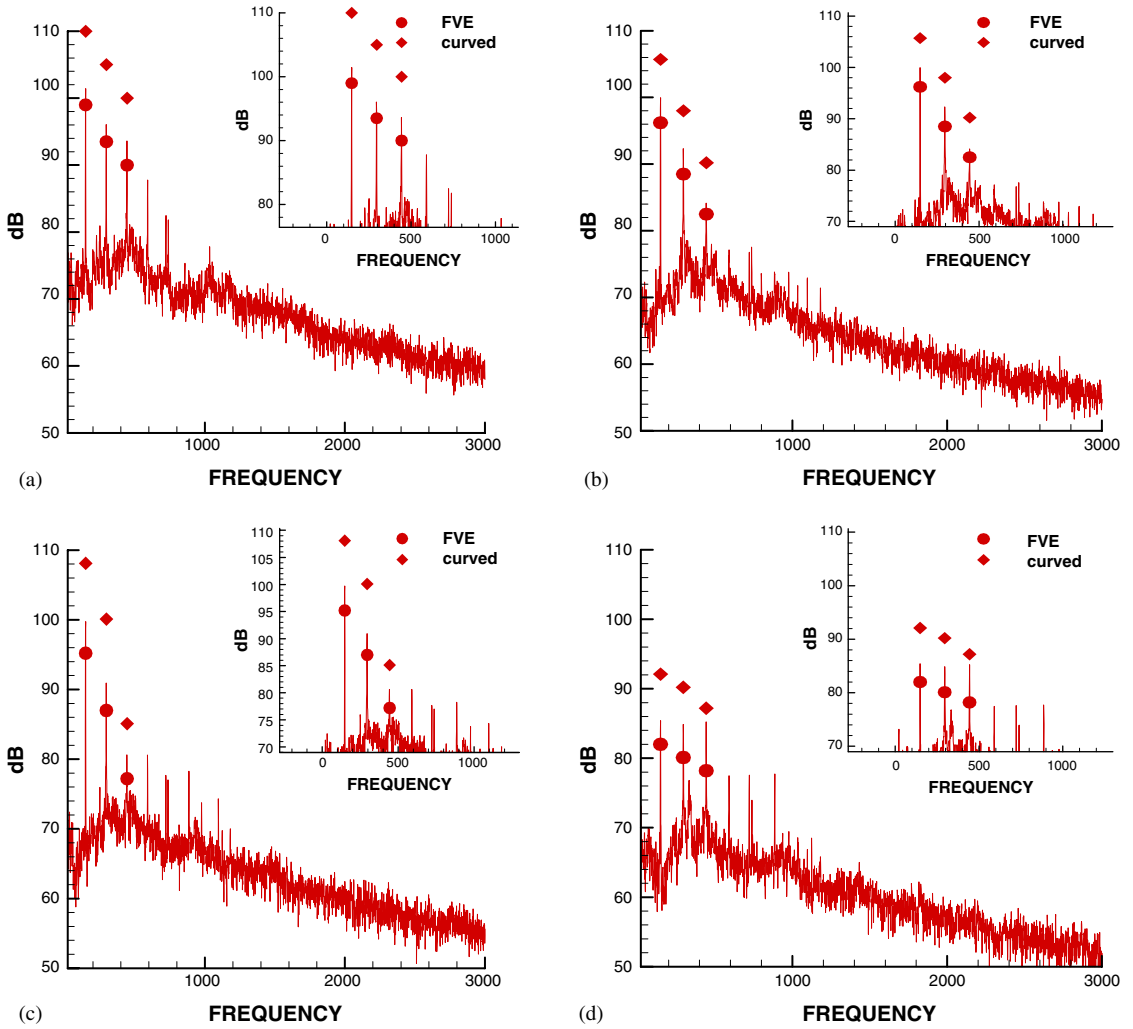


Fig. 7. Comparison of calculation results with measurement data: (a) point 1; (b) point 2; (c) point 3; (d) point 4.

spectra are plotted with the experimental results in Fig. 7. Fig. 7 shows that results by a curved vortex analysis overestimate BPF components. The resulting noise predictions by FVE underestimate a discrete noise, but these have more favorable agreements with measurement data. It is attributed that since the wake–vane interaction by the FVE makes $C_p$ difference lesser than curved vortex results and have dull spike in $C_p$ peaks as shown in Fig. 5, these results let the discrete noise level by FVE analysis lesser but more accurate than by the curved vortex analysis. Thus, it is thought that FVE is more effective flow analysis tool in such a case where the blade–vane interaction has to be considered.

### 3.2. Fan design

With this FVE flow analysis tool, a blade planform design is carried out. Design variables are alternations of leading edges and trailing edges of fan blades that are basically indicated by Hicks and Henne (HH) [17] shape function, i.e. each displacement of leading edges and trailing edges and each position of the maximum displacement are indicated with $x_1$, $x_2$, $x_3$, $x_4$.

$$y = y_{\text{base}} + \sum_{k=1}^{n_v} w(x_k) \cdot f_k,$$

where $f_k = \sin[\pi x^{e(k)}]^3$, $e(k) = \ln(0.5)/\ln(x_k)$.

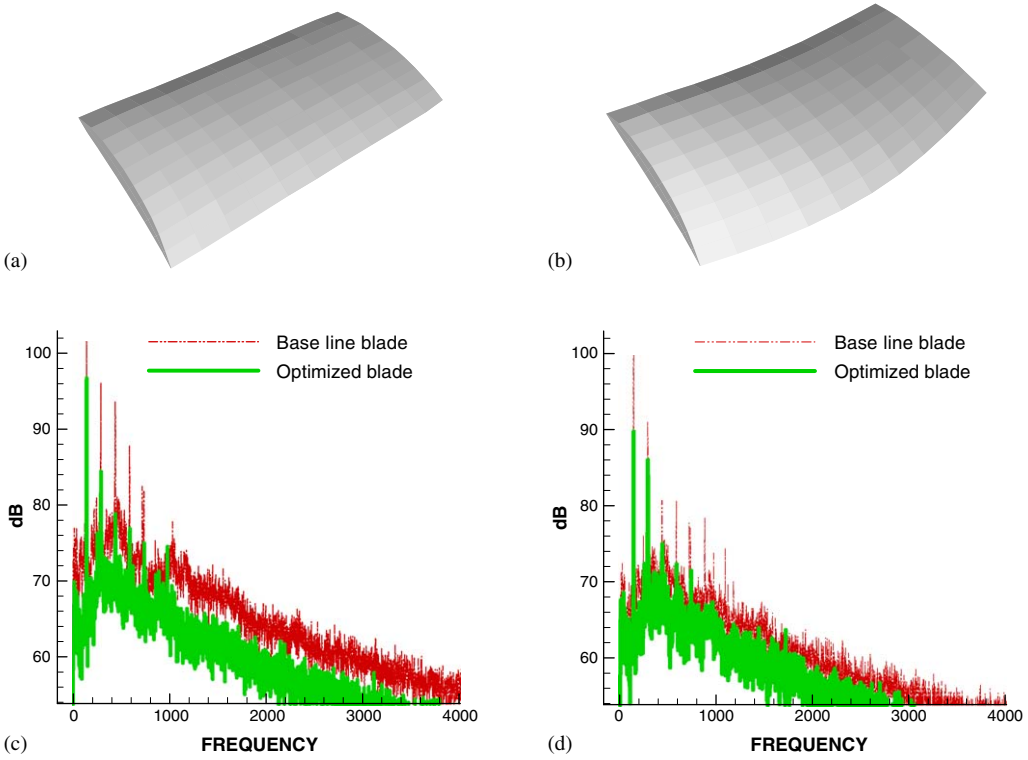


Fig. 8. Blade planform and noise comparison of the base line blade with the optimized blade: (a) base line blade; (b) optimized blade; (c) comparison at point 1; (d) comparison at point 2.

Table 3
Blade geometry factors

| | $w/R$ | $x_k/R$ |
|---|---|---|
| Leading edge | 0.03 | 0.51 |
| Trailing edge | 0.05 | 0.48 |

The leading edges and trailing edges change by the shape function. A response surface is constructed from four design variables of the blade shape which is built by this method.

In order to form the response surface, the performance and noise are analyzed by the FVE model and acoustic analogy. Data are acquired after performing 5-revolution numerical simulation (60 calculations per 1 revolution) in order to have proper accuracy, then the pressure fluctuation of blade surface are successively obtained, and finally applied to acoustic analysis.

Even though the flow-field analysis and the noise prediction methodology used in this study are relatively much faster than other methods, such as CFD methods, it requires considerable amount of time for each case. Therefore, 30 numerical experimental points was chosen by D-optimal condition [10], and then the performance and noise were calculated with a variation of the shape of the blade. However, to simplify the problem the object function is selected as the following in a way of increasing flow rate but reducing noise.

$$\text{Minimize} \quad w_i(10 * \text{dB}) + (1 - w_i)(-\dot{V}),$$

where $0 \leqslant w_i \leqslant 1$.

The object function for noise was multiplied by 10, in order to equalize the scale with the object function of flow rate.

The resultant shape of the blade after the optimization and the comparisons of the optimized blade with the baseline blade for noise spectrum are shown in Fig. 8(a) and (b), respectively. In Table 3, optimized blade geometry factors are described. As shown in Fig. 8(c) and (d), the noise was diminished as much as 8 dB(A) at 2 m from fan hub while the flow rate and the efficiency are maintained as those of the baseline blade.

## 4. Conclusion

A new free wake model, named as FVE, is developed to apply an axial fan blade design. FVE model, on the contrary to a conventional free wake model, enables us to simulate the blade–wake–guide vane interaction by cutting a vortex filament when the vortex filament collides with a guide vane. The comparison of measured sound data of a prototype fan with the calculated results implies the validity of the proposed numerical method. However, the calculation does not provide satisfactory results in the high frequency region due to the Nyquist frequency limitation.

This new free wake model combined with RSM design technique provides an efficient way to design an optimized blade planform for lower noise, and then the final design gives a reduction of 8 dB(A) at 2 m from fan hub in the overall noise level. This result shows a devised FVE methodology has a potential as an efficient and effective tool for fan design.

## References

[1] M.J. Sheu, Numerical investigation of design parameters for an axial flow cooling fan, SAE Paper 970933 (1997).
[2] S. Moreau, S. Caro, Aeroacoustic modelling of low pressure axial flow fans design, *sixth AIAA/CEAS Aeroacoustics Conference*, AIAA Paper 2000-2094, Lahaina, Hawaii, 2000.
[3] J. Ahn, Comparison of Design Optimization Methods in the Flowfields with Non-Smooth or Noisy Functions, PhD Dissertation, Department of Aerospace Engineering, Seoul National University, 2000.
[4] D. B., Bliss, T. R., Quackenbush, A. J., Bilanin, A new methodology for helicopter free wake analyses, *39th Annual Forum of the American Helicopter Society*, May 1983.
[5] W.J. McCroskey, Vortex wakes of rotorcraft, *33rd Aerospace Sciences Meeting and Exhibit*, January 1995.
[6] T.R. Quackenbush, D.B. Bliss, D.A. Wachspress, New free-wake analysis of rotorcraft hover performance using influence coefficient'', *Journal of Aircraft* 26 (12) (1989).
[7] T.R. Quackenbush, D.B. Bliss, D.A. Wachspress, C.C. Ong, Free-wake analysis of hover performance using a new influence coefficient method, NASA CR 4309, 1990.
[8] Jeonghan Lee, Analysis and Optimization of Aerodynamic Noise in Axial Flow Fan, PhD Dissertation, School of Mechanical and Aerospace Engineering, Seoul National University, 2001.
[9] A.G. Anthony, Aircraft Multidisciplinary Design Optimization Using Design of Experimental Theory and Response Surface Modeling Methods, PhD Dissertation, Department of Aerospace Engineering, Virginia Polytechnic, Institute and State University, Blackburg, VA, 1997.
[10] V.R. Hogg, J. Ledolter, *Applied Statistics for Engineers and Physical Scientists*, second ed., Macmillan Publishing Company, New York, 1992.
[11] S. B. Kenneth prediction of helicopter rotor discrete frequency noise, NASA Technical Memorandum 87721.
[12] J.E. Ffowcs Williams, D.L. Hawkings, Sound generation by turbulence and surfaces in arbitrary motions, *Philosophical Transactions of the Royal Society London, Series A* 264 (1151) (1969).
[13] M.J. Lighthill, On sound generated aerodynamically. I. General theory, *Proceedings of the Royal Society of London, Series A* 211 (1107) (1952).
[14] F. Farassat, G.P. Succi, The prediction of helicopter rotor discrete frequency noise, *Vertica* 7 (4) (1983).
[15] F. Farrasat, Theory of noise generation from moving bodies with an application to helicopter rotors, NASA TR R-451, 1975.
[16] A.W. Daniel, R.Q. Todd, BVI noise prediction using a comprehensive rotorcraft analysis, *AHS 57th Annual Forum*, Washington, DC USA, 2001.
[17] R.M. Hicks, P.A. Henne, Wing design by numerical optimization, *Journal of Aircraft* 15 (7) (1978) 407–412.